DYNAMIC MODE ANALYSIS OF TIDAL FLOWS THROUGH THE STRAIT OF GIBRALTAR

Sathsara Dias, Kanaththa Priyankara, **Sudam Surasinghe**, Marko Budišić, Erik Bollt

Clarkson Center for Complex Systems Science, Clarkson University

Ocean Dynamics of the Strait of Gibraltar

Dynamics of oceans can be modeled by a complex, nonlinear set of equations. Oceanographic features (currents, eddies, etc.) arise from first-principle models, and interact in a nonlinear, time-dependent, and complex ways.

Several oceanographic features play a prominent role in the Strait of Gibraltar and Alboran Sea that lies to the east of it:

Western Alboran Gyre: Anti-cyclonic eddy located at the entrance of the Mediterranean.

Camarinal Sill: Site of an internal hydraulic jump, giving rise to internal waves comprising solitons and internal tides.

Propagating wave trains: Originating at the Camarinal Sill, these long-lived waves are observable deeper in the Mediterranean.

Objective: The Strait of Gibraltar has a number of interesting features, including waves that are generated by a combination of flow over topography and tides. We are interested in how much of this can be captured by the (linear) DMD method.

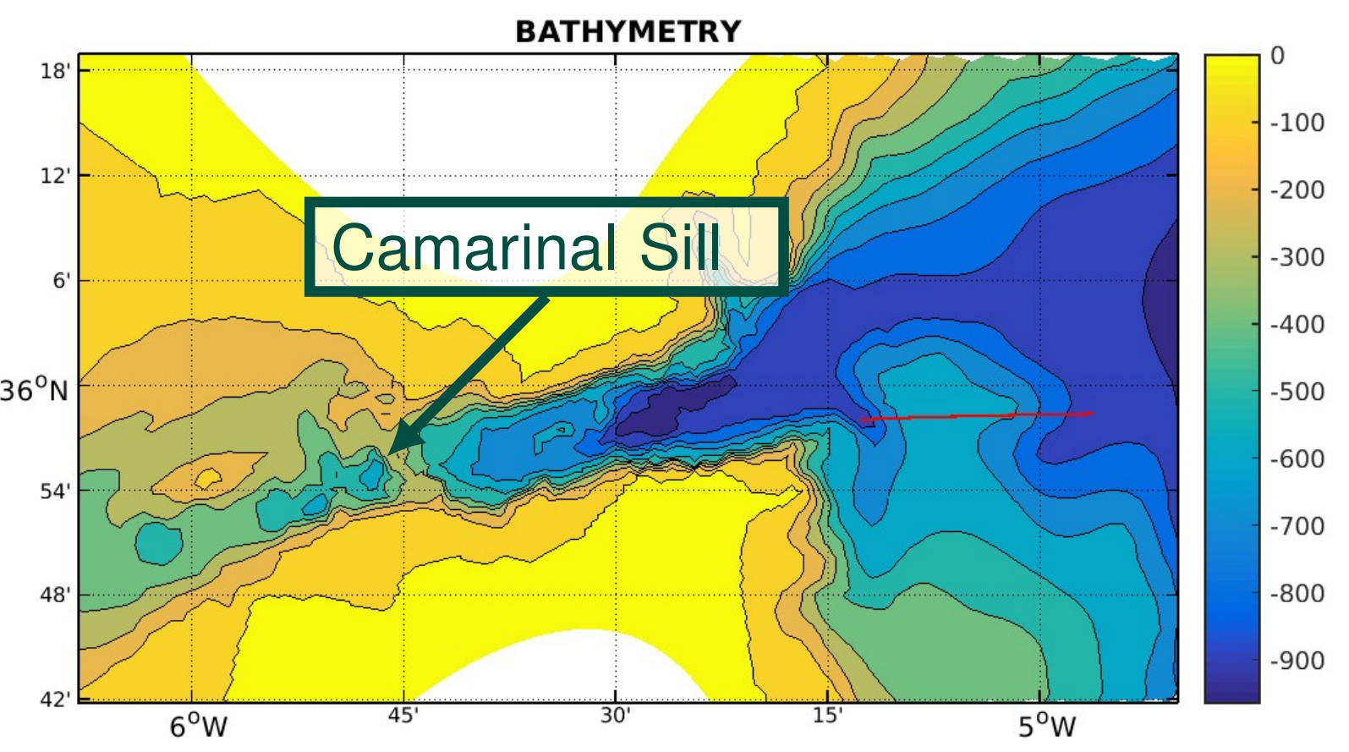

Fig. 1: Sea depth in the Strait of Gibraltar

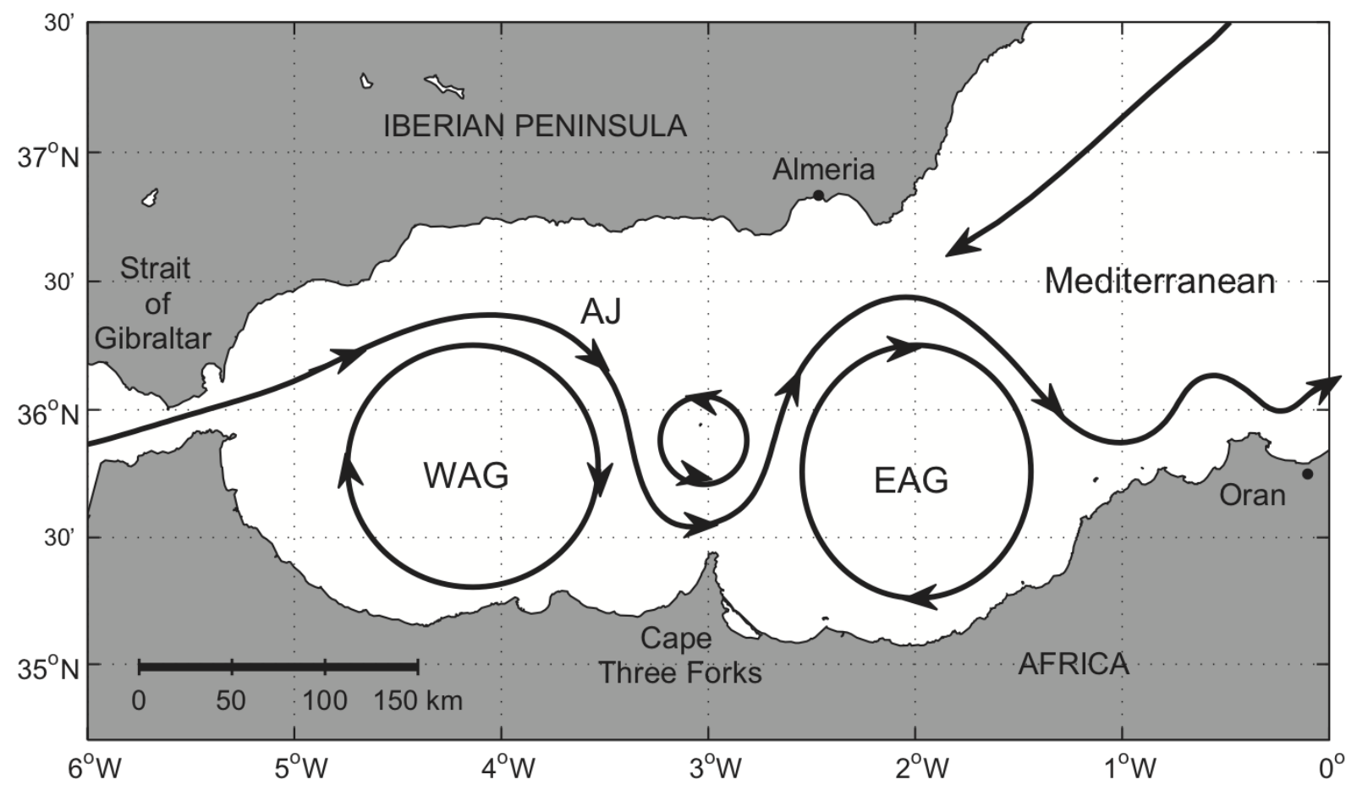

Fig. 2: Sketch of typical features in Alboran sea, reprinted from [1].

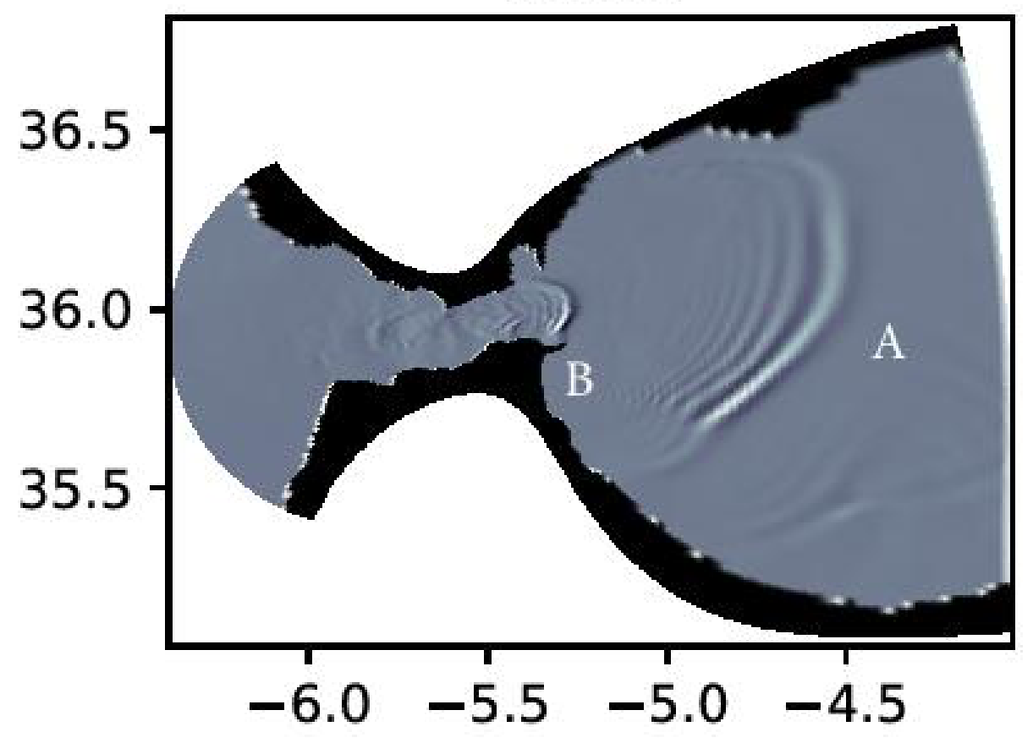

Fig. 3: Propagation (A) and birth (B) of internal waves.

Numerical model

Numerical model of the ocean dynamics, described in [1], captures all relevant tidal constituents. The tide in the Strait of Gibraltar is semi-diurnal. Its most important constituents are, in order of importance, M2, S2, N2, and K2 [2]. The tidal mode M2 is the principal lunar semi-diurnal tidal, with the period of 12.42 hours. Tidal mode S2 is the principal solar semi-diurnal tidal and its period is 12 hours.

The simulated data set that was provided by Jose C. Sánchez-Garrido is a three-dimensional, time-resolved model. The simulation covers 6 days, in 144 snapshots ($\Delta t = 1$ hour). The spatial grid is based on the Northern Hemisphere intermediate resolution model, covering 32 depth levels and 190×96 longitude/latitude nodes with approximately $500\mathrm{m}$ step size, roughly covering the area in Fig. 1.

Dynamic Mode Decomposition (DMD)

Koopman operator [3] is a linear, ∞-dimensional model of nonlinear dynamics that propagates measurement functions g along evolution of dynamics under flow map S_t $\mathbb{K}_t[g](x) = g(S_t(x))$.

DMD is a numerical algorithm for eigendecomposition of $\mathbb{K}$, without explicit approximation of the entire $\mathbb{K}$ [4]. Depending on the purpose of the application, there are a few variations of the basic algorithm. In this project we used the *standard* DMD algorithm [5].

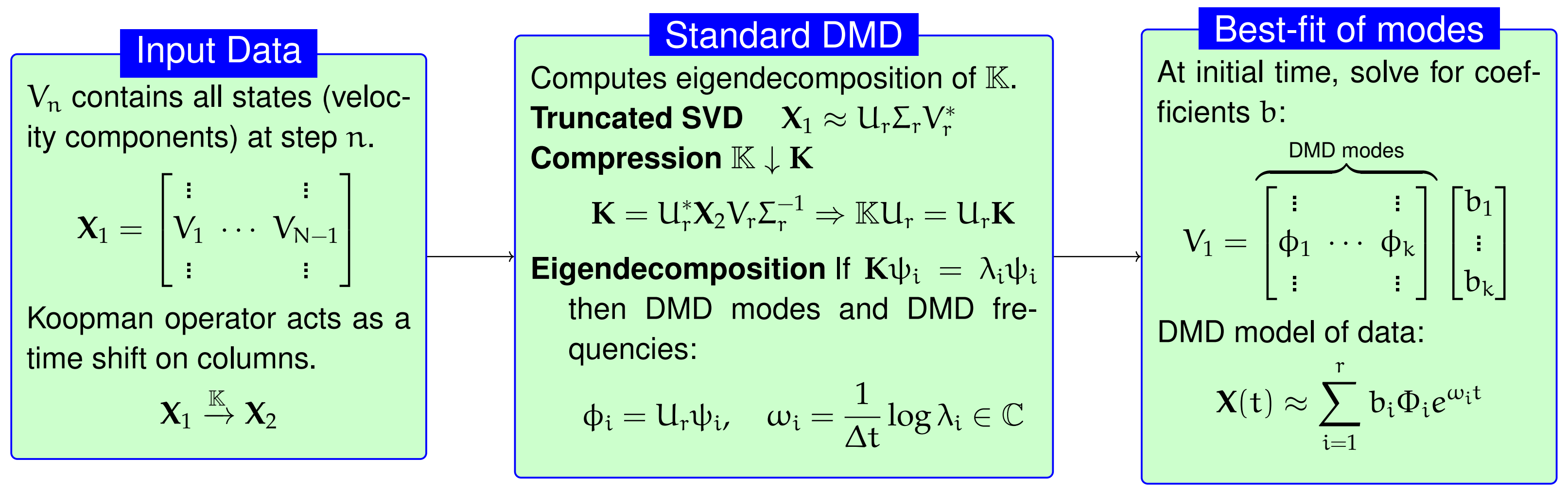

Input Data

V_n contains all states (velocity components) at step n.

$$\mathbf{X}_1 = \begin{bmatrix} \vdots & & \vdots \\ V_1 & \cdots & V_{N-1} \\ \vdots & & \vdots \end{bmatrix}$$

Koopman operator acts as a time shift on columns.

$$\mathbf{X}_1 \xrightarrow{\mathbb{K}} \mathbf{X}_2$$

Standard DMD

Computes eigendecomposition of $\mathbb{K}$.

Truncated SVD $\mathbf{X}_1 \approx U_r \Sigma_r V_r^*$

Compression $\mathbb{K} \downarrow \mathbf{K}$

$$\mathbf{K} = U_r^* \mathbf{X}_2 V_r \Sigma_r^{-1} \Rightarrow \mathbb{K} U_r = U_r \mathbf{K}$$

Eigendecomposition If $\mathbf{K}\psi_i = \lambda_i \psi_i$ then DMD modes and DMD frequencies:

$$\phi_i = U_r \psi_i, \quad \omega_i = \frac{1}{\Delta t} \log \lambda_i \in \mathbb{C}$$

Best-fit of modes

At initial time, solve for coefficients b:

$$V_1 = \overbrace{\begin{bmatrix} \vdots & & \vdots \\ \phi_1 & \cdots & \phi_k \\ \vdots & & \vdots \end{bmatrix}}^{\text{DMD modes}} \begin{bmatrix} b_1 \\ \vdots \\ b_k \end{bmatrix}$$

DMD model of data:

$$\mathbf{X}(t) \approx \sum_{i=1}^{r} b_i \Phi_i e^{\omega_i t}$$

DMD spectrum associated with tides

Mode selection done by time averaged L_2 norm contribution, $E_i = \frac{1}{T}\int_0^T \|b_i e^{\omega_i t}\|^2 dt$. If the ratio of the tidal and mode period is an integer we consider them related.

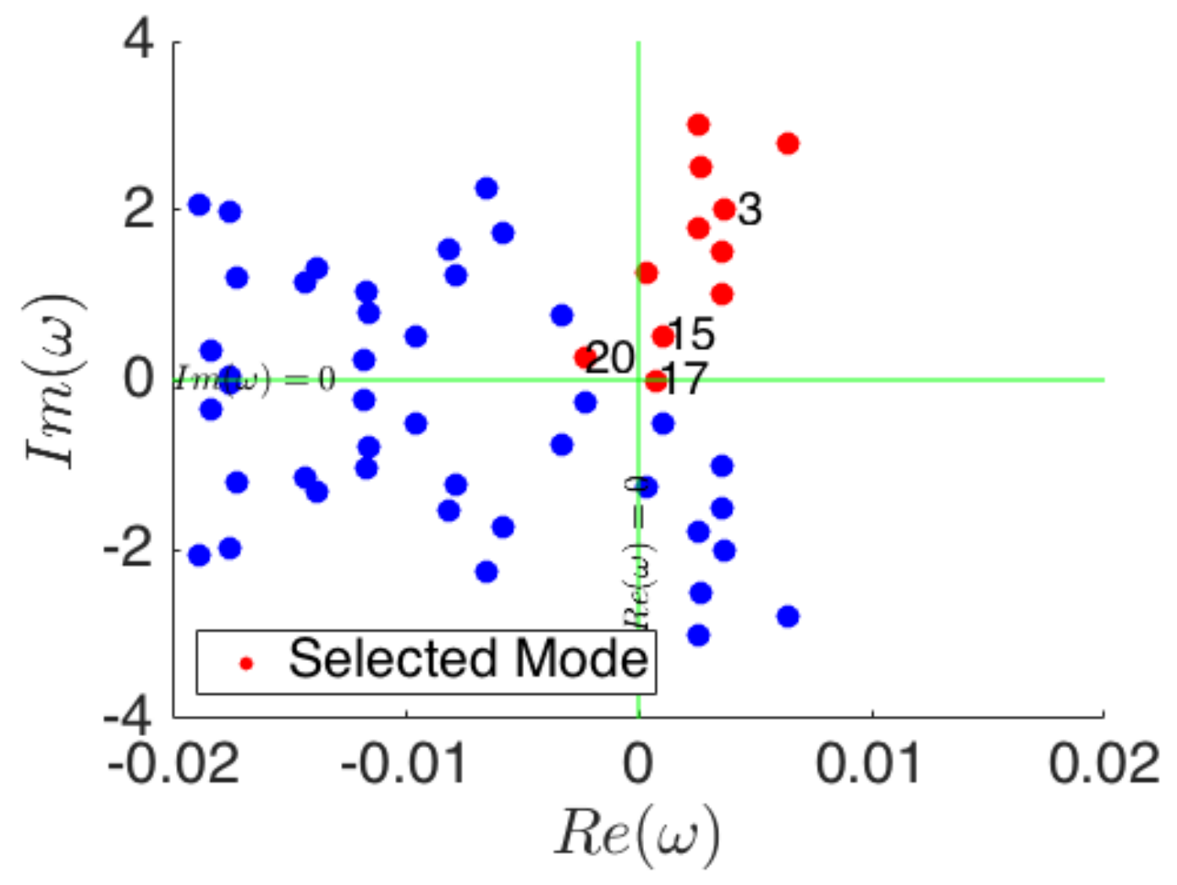

(a) DMD eigenvalues in complex plane

Mode	$\frac{1}{2}$ or $2\times$ time (h)	Period (h)	$\frac{\text{Tide}}{\text{Mode}}$ period ratio	Related Tide
1	-108.42	2.26		
3	-185.83	3.13	3.97	M2
5	-191.33	4.17	2.98	M2
7	-194.72	6.25	1.99	M2
9	-264.13	3.51		
11	-260.28	2.50	4.97	M2
13	-274.23	2.09	2.95	M2
15	-630.60	12.12	0.99	S2
17	-894.93	∞		
18	-2000	4.92		
20	302.2	24.29	0.49	S2

(b) Time constants of DMD modes. Negative growth/decay values indicate growing modes.

Fig. 5: DMD eigenvalues and associated features

Dynamics of modes depend on eigenvalues ω_i, with stability governed by the real and periodicity by imaginary part of the ω. If $\mathrm{Im}(\omega_i) \neq 0$ then mode will have a oscillatory behavior. If $\mathrm{Re}(\omega_i)$ is negative then mode will die out otherwise mode will grow. Decaying modes are labeled by half-life, time to reach half the original value, while growing modes correspondingly have doubling time.

Result: DMD isolates tidal components

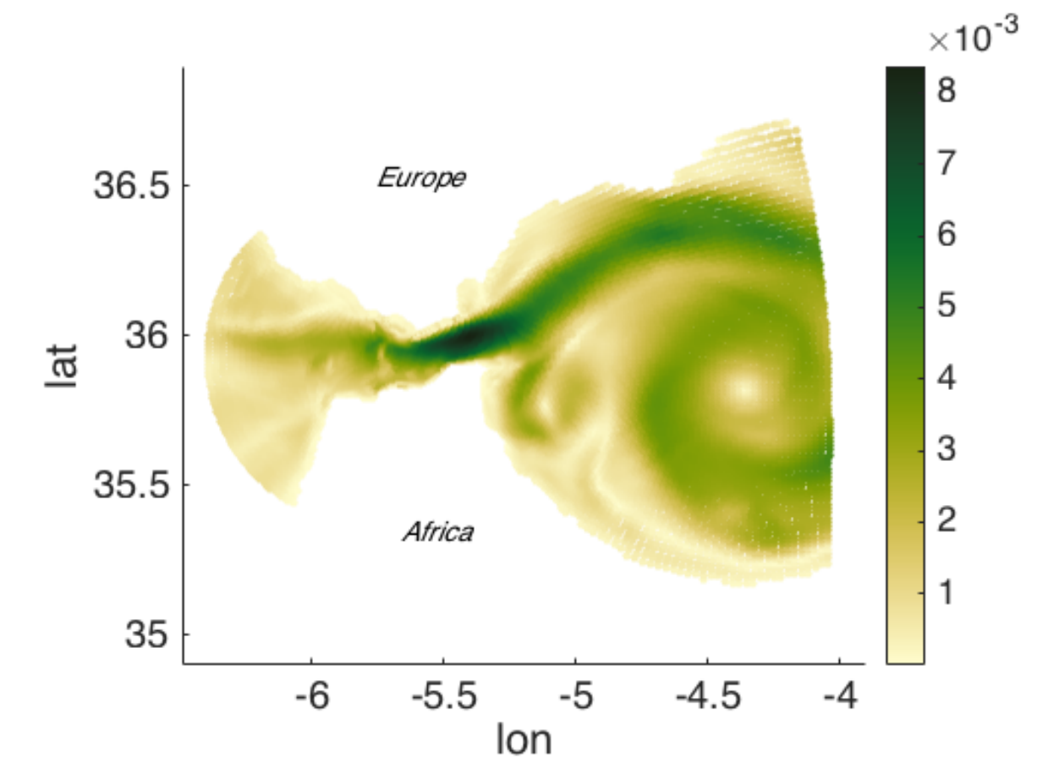

Fig. 6: Ocean surface speed profile of mean flow (DMD mode 17).

The mode 17 captures the Western Alboran Gyre. Notice that $\mathrm{Im}\,\omega_{17} = 0$. Therefore this mode is approximately non-oscillatory. Over the course of this simulation, this mode grows with doubling time around 37 days (894 hours).

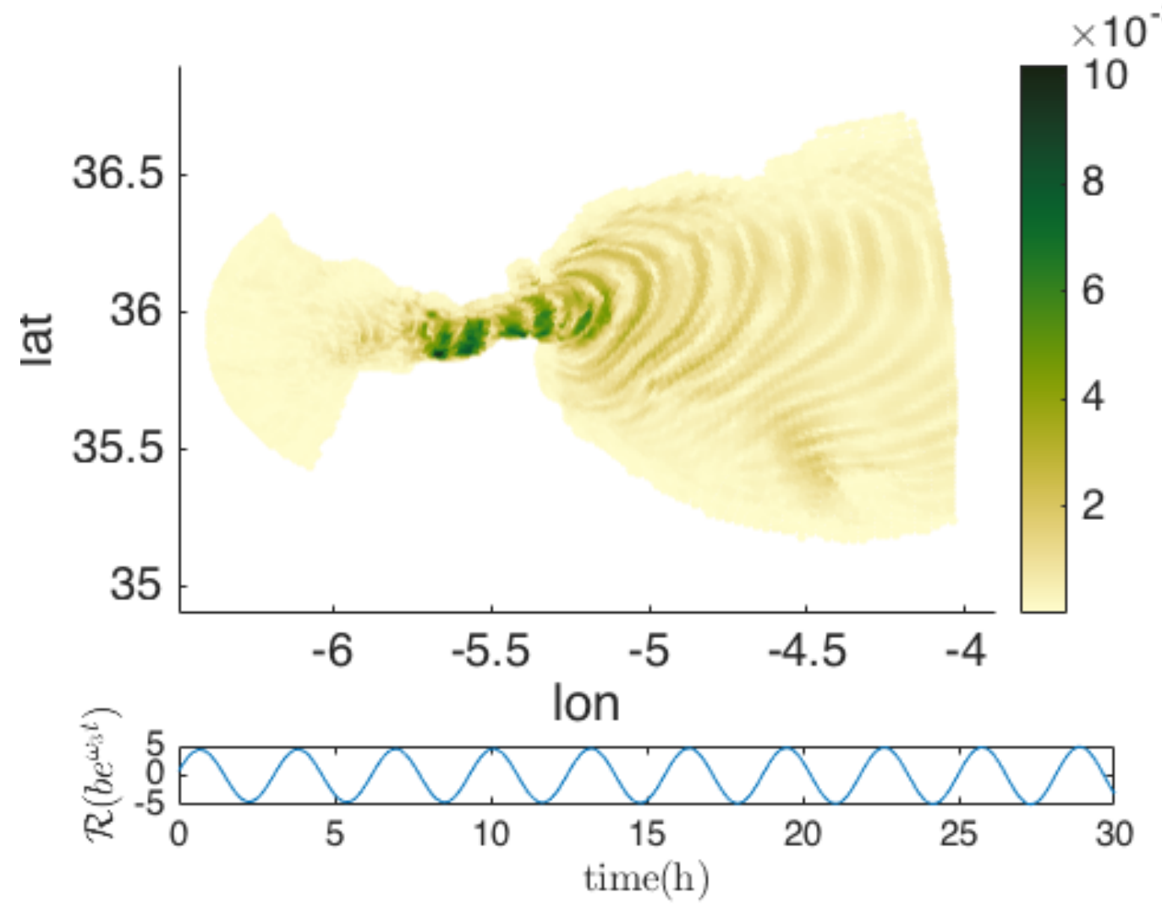

Fig. 7: Ocean surface speed profile of Mode 3.

DMD modes which related to the principal lunar semidiurnal (M2) tidal modes, capture the internal wave train A (Fig. 3). These are periodic modes.

Time-periodic DMD modes which closely related to principal solar semidiurnal (S2) tidal mode, capture the internal wave train B (Fig. 3).

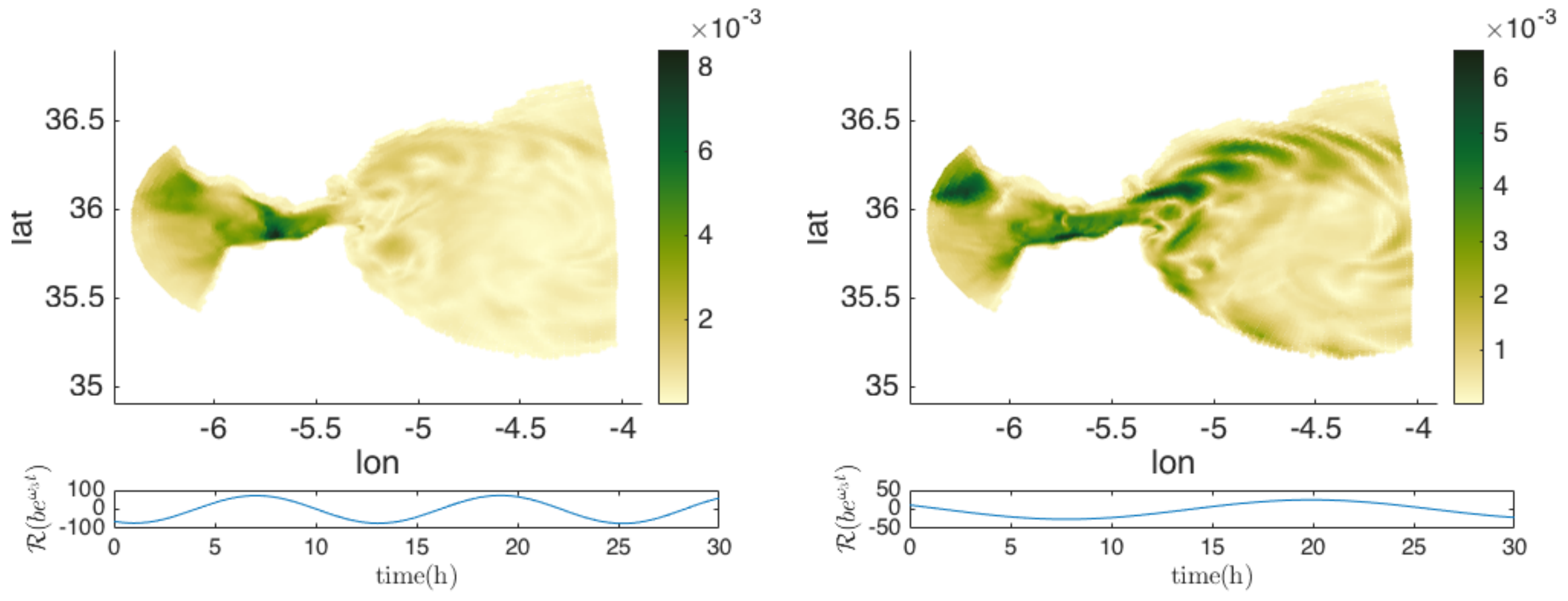

(a) Mode 15

(b) Mode 20

Fig. 8: Modes associated with semidiurnal (S2) tides. Ocean surface speed profile.

Acknowledgments: We thank Larry J. Pratt (Woods Hole Institute) and Jose C. Sánchez-Garrido (U. of Malaga) for the simulated data set and helpful discussions.

[1] J. C. Sánchez-Garrido, J. G. Lafuente, E. Álvarez Fanjul, M. G. Sotillo, and F. J. de los Santos, “What does cause the collapse of the western alboran gyre? results of an operational ocean model”, Progress in Oceanography **116**, 142 –153 (2013).

[2] J. G. Lafuente, J. Almazán, F Castillejo, A Khribeche, and A Hakimi, “Sea level in the strait of gibraltar: tides”, The International Hydrographic Review **67** (1990).

[3] M. Budišić, R. Mohr, and I. Mezić, “Applied Koopmanism”, Chaos. An Interdisciplinary Journal of Nonlinear Science **22**, 047510, 33 (2012).

[4] C. W. Rowley, I. Mezić, S. Bagheri, P. Schlatter, and D. S. Henningson, “Spectral analysis of nonlinear flows”, Journal of Fluid Mechanics **641**, 115–127 (2009).

[5] J. N. Kutz, S. L. Brunton, D. M. Luchtenburg, C. W. Rowley, and J. H. Tu, “On dynamic mode decomposition: theory and applications”, Journal of Computational Dynamics **1**, 391–421 (2014).